

Effects of Convection and Diffusion on Rational Reduction of Detailed Kinetic Schemes

Sandeep Singh, Joseph M. Powers*, and Samuel Paolucci
Department of Aerospace and Mechanical Engineering,
University of Notre Dame,
Notre Dame, Indiana 46556-5637

Abstract

This work addresses the construction of slow manifolds for chemically reactive flows. The construction relies on the same decomposition of a local eigensystem that is used in the formation of what are known as Intrinsic Low Dimensional Manifolds (ILDMs). We give an improved extension of the standard ILDM method to systems where reaction couples with convection and diffusion. Reduced model equations are obtained by equilibrating the fast dynamics of a closely coupled reaction/convection/diffusion system and resolving only the slow dynamics of the same system in order to reduce computational costs, while maintaining a desired level of accuracy. The improvement is realized through formulation of an elliptic system of partial differential equations which describe the infinite-dimensional Approximate Slow Invariant Manifold (ASIM) for the reactive flow system. Enhanced accuracy is demonstrated for a premixed laminar flame in ozone where it is shown that the error in flame speed incurred using the ASIM is much less than that incurred by using a Maas-Pope Projection (MPP) to account for convection and diffusion.

Introduction

A wide variety of combustion processes involve a large number of elementary reactions occurring simultaneously within a complex flow field. These processes are modeled by a large number of partial differential equations (PDEs) representing the evolution of numerous reactive chemical species, coupled with the full Navier-Stokes equations. Fully resolved solution of these model equations, which incorporate detailed finite rate chemical kinetics, often requires a prohibitive amount of computational resources. Hence, there is a need to develop methods which rationally reduce the model equations so that numerical simulations can be accomplished in a reasonable computational time. Elementary chemical reactions occur over a wide range of time scales which is manifested as stiffness in the model equations, which induces high computational costs. For stable systems, this stiffness can be reduced by equilibrating the fast time scale chemical processes and resolving only the relevant slow time scale processes. The reduced model equations describe the slow dynamics under the assumption that the fast dynamics can be neglected. Most chemical time scales are faster than time scales associated with fluid mechanical phenomenon such as convection and diffusion. Nevertheless, it is important that the reduced model equations maintain the coupling of the flow processes with those chemi-

cal processes which occur at similar time scales. In this work we illustrate how this coupling of fluid and chemical processes can be maintained such that an approximate and less expensive numerical solution of the reduced model equations is consistent with the more accurate and expensive numerical solution of the full model equations.

The method of Intrinsic Low Dimensional Manifolds (ILDM) [1] uses a dynamical systems approach of time scale analysis to systematically reduce the stiffness introduced by chemistry. The method is developed for spatially homogeneous premixed reactive systems (in the absence of any transport processes such as convection and diffusion), which can be modeled by systems of ordinary differential equations (ODEs). The behavior of these reactive systems can be described by trajectories in the associated phase space starting from an initial condition and relaxing to a chemical equilibrium.

The ILDM is only an approximation of what we call the Slow Invariant Manifold (SIM). For spatially homogeneous systems, both the ILDM and the SIM have finite dimension. Relative to the more fundamental SIM, the ILDM contains a small intrinsic error for large finite stiffness. The SIM describes the slow dynamics of the spatially homogeneous reactive systems more accurately. However, provided that a spectral gap condition is satisfied, the ILDM does a good job of approximating the SIM, and in our experience, computation of high dimensional ILDMs appears to be more tractable than that of high di-

*Corresponding author: powers@nd.edu
Proceedings of the Third Joint Meeting of the U.S. Sections of
The Combustion Institute

note that the basis \mathbf{V} is derived solely from the chemistry of the spatially homogeneous system. While this will lead to an improved estimation of the system's behavior, a better basis on which to project would take account of the infinite-dimensional eigenfunctions associated with the Jacobian of the convection-diffusion operator. This, however, is difficult.

We can then rewrite Eq. (1) as

$$\frac{1}{\lambda_{(i)}} \left(\frac{\partial z_i}{\partial t} + \tilde{\mathbf{v}}_i \sum_{j=1}^n \frac{\partial \mathbf{v}_j}{\partial t} z_j \right) = z_i + \frac{1}{\lambda_{(i)}} (\tilde{\mathbf{v}}_i \mathbf{g}) - \frac{1}{\lambda_{(i)}} \left(\tilde{\mathbf{v}}_i \frac{\partial \mathbf{h}}{\partial x} \right), \quad i = 1, \dots, n. \quad (3)$$

Here \mathbf{g} is defined as the nonlinear part of \mathbf{f} : $\mathbf{g} = \mathbf{f} - \mathbf{J}\mathbf{y}$. We assume that we are only interested in the dynamics of the processes occurring at time scales of $\frac{1}{|\lambda_{(m)}|}$ or slower and that a spectral gap exists. Hence, we assume that all other processes occurring at faster time scales are equilibrated by setting to zero the left hand side of Eq. (3) for $i = m + 1, \dots, n$, which is $\mathcal{O}\left(\frac{1}{|\lambda_{(m+1)}|}\right)$ or smaller, while the right hand side is $\mathcal{O}(1)$ or larger for the same. Hence, the following is obtained

$$z_i + \frac{1}{\lambda_{(i)}} (\tilde{\mathbf{v}}_i \mathbf{g}) - \frac{1}{\lambda_{(i)}} \left(\tilde{\mathbf{v}}_i \frac{\partial \mathbf{h}}{\partial x} \right) = 0, \quad i = m + 1, \dots, n. \quad (4)$$

If convection and diffusion processes occur at time scales which are slower than reaction time scales of order $\frac{1}{|\lambda_{(m+1)}|}$, then we can neglect the third term in Eq. (4), as it becomes $\mathcal{O}\left(\frac{1}{|\lambda_{(m+1)}|}\right)$ or smaller while the remaining terms are $\mathcal{O}(1)$ or larger. Instead, if convection and diffusion time scales overlap with fast chemical time scales, then we cannot make such an approximation as the third term in Eq. (4) will become $\mathcal{O}(1)$ or larger. No robust analysis exists to determine convection and diffusion time scales *a priori*. We assume that convection and diffusion processes occur at time scales of $\frac{1}{|\lambda_{(p)}|}$ for $m < p < n$ and slower. Then by equilibrating the fast dynamics, we obtain the differential algebraic system of equations given by

$$z_i + \frac{1}{\lambda_{(i)}} (\tilde{\mathbf{v}}_i \mathbf{g}) - \frac{1}{\lambda_{(i)}} \left(\tilde{\mathbf{v}}_i \frac{\partial \mathbf{h}}{\partial x} \right) = 0, \quad i = m + 1, \dots, p, \quad (5a)$$

$$z_i + \frac{1}{\lambda_{(i)}} (\tilde{\mathbf{v}}_i \mathbf{g}) = 0, \quad i = p + 1, \dots, n. \quad (5b)$$

These equations can be rewritten in a more convenient form as

$$\tilde{\mathbf{V}}_{fs} \mathbf{f} - \tilde{\mathbf{V}}_{fs} \frac{\partial \mathbf{h}}{\partial x} = \mathbf{0}, \quad (6a)$$

$$\tilde{\mathbf{V}}_{ff} \mathbf{f} = \mathbf{0}, \quad (6b)$$

where now

$$\tilde{\mathbf{V}}_f = \begin{pmatrix} - & \tilde{\mathbf{v}}_{m+1} & - \\ & \vdots & \\ - & \tilde{\mathbf{v}}_p & - \\ & \tilde{\mathbf{v}}_{p+1} & - \\ & \vdots & \\ - & \tilde{\mathbf{v}}_n & - \end{pmatrix} = \begin{pmatrix} - & \tilde{\mathbf{V}}_{fs} & - \\ & \tilde{\mathbf{V}}_{ff} & \end{pmatrix}, \quad (7)$$

where the matrix $\tilde{\mathbf{V}}_{fs}$ has dimension $(p - m) \times n$ and its row vectors contain the reciprocal vectors of the right eigenvectors associated with the time scales $\frac{1}{|\lambda_{(m+1)}|}, \dots, \frac{1}{|\lambda_{(p)}|}$, and the matrix $\tilde{\mathbf{V}}_{ff}$ has dimension $(n - p) \times n$ and its row vectors contain the reciprocal vectors of the right eigenvectors associated with the time scales $\frac{1}{|\lambda_{(p+1)}|}, \dots, \frac{1}{|\lambda_{(n)}|}$. Equations (6) represent the *infinite-dimensional* Approximate Slow Invariant Manifold (ASIM) on which the slow dynamics occurs once all fast time scale processes have equilibrated. They correspond to a system of differential algebraic equations which have to be solved together with prescribed boundary conditions. Hence, the slow dynamics for Eq. (1) is approximated by integrating the following set of partial differential algebraic equations:

$$\tilde{\mathbf{V}}_s \frac{\partial \mathbf{y}}{\partial t} = \tilde{\mathbf{V}}_s \mathbf{f} - \tilde{\mathbf{V}}_s \frac{\partial \mathbf{h}}{\partial x}, \quad (8a)$$

$$\mathbf{0} = \tilde{\mathbf{V}}_{fs} \mathbf{f} - \tilde{\mathbf{V}}_{fs} \frac{\partial \mathbf{h}}{\partial x}, \quad (8b)$$

$$\mathbf{0} = \tilde{\mathbf{V}}_{ff} \mathbf{f}. \quad (8c)$$

The reduced PDEs in Eq. (8a) describe the time evolution of the slow dynamics, and are solved in conjunction with Eqs. (8b) and (8c) describing the ASIM. The ASIM is an infinite dimensional manifold which accounts for the effects of convection and diffusion. The stiffness due to the reaction source term in Eq. (1) is substantially reduced in Eqs. (8). It is obvious that for two- and three-dimensional reactive flow equations the ASIM is described by a set of elliptic partial differential algebraic equations.

Premixed Laminar Flame for Ozone Decomposition

The governing equations which model the time-dependent, one-dimensional, isobaric, premixed lam-

inar flame for ozone decomposition in Lagrangian coordinates are derived from the Navier-Stokes equations under the assumptions of low Mach number [5],

$$\frac{\partial T}{\partial t} + \dot{m}_0 \frac{\partial T}{\partial \psi} = -\frac{1}{\rho c_p} \sum_{k=1}^3 \dot{\omega}_k M_k h_k + \frac{1}{c_p} \frac{\partial}{\partial \psi} \left(\rho \lambda \frac{\partial T}{\partial \psi} \right) + \sum_{k=1}^3 \frac{c_p^k}{c_p} \rho^2 \mathcal{D}_k \frac{\partial Y_k}{\partial \psi} \frac{\partial T}{\partial \psi}, \quad (9a)$$

$$\frac{\partial Y_k}{\partial t} + \dot{m}_0 \frac{\partial Y_k}{\partial \psi} = \frac{1}{\rho} \dot{\omega}_k M_k + \frac{\partial}{\partial \psi} \left(\rho^2 \mathcal{D}_k \frac{\partial Y_k}{\partial \psi} \right), \quad (9b)$$

$k = 1, 2, 3,$

where the dependent variables are the fluid temperature T and the mass fractions in the fluid mixture, Y_1 , Y_2 and Y_3 , of the oxygen atom O , the oxygen molecule O_2 and the ozone molecule O_3 , respectively. The terms M_k and c_p^k represent the molecular mass and the specific heat capacity at constant pressure, respectively, of species k . The mass averaged specific heat capacity at constant pressure of the fluid mixture is given by

$$c_p = \sum_{k=1}^3 Y_k c_p^k. \quad (10)$$

The specific enthalpy of species k is given by

$$h_k = h_{0k} + \int_{T_0}^T c_p^k(\tilde{T}) d\tilde{T}, \quad (11)$$

where h_{0k} is the standard enthalpy of formation per unit mass of species k at the standard temperature $T_0 = 298$ K. The mass diffusion coefficient of species k into the fluid mixture is \mathcal{D}_k , while the thermal conductivity of the fluid mixture is λ . The mixture density is ρ . The independent variables are time t , and the Lagrangian coordinate ψ , where

$$\psi(t, x) = \int_0^x \rho(t, \tilde{x}) d\tilde{x}, \quad (12)$$

where x is the spatial coordinate. The inlet mass flow rate, \dot{m}_0 , is given by

$$\dot{m}_0(t) = \rho u|_{x=0}, \quad (13)$$

where u is the flow velocity. The molar rate of production of species k per unit volume, $\dot{\omega}_k$, is given by the law of mass action with Arrhenius kinetics

$$\dot{\omega}_k = \sum_{j=1}^J a_j T^{\beta_j} e^{\left(\frac{-E_j}{\Re T}\right)} (\nu''_{kj} - \nu'_{kj}) \prod_{i=1}^N \left(\frac{\rho Y_i}{M_i}\right)^{\nu'_{ij}}, \quad (14)$$

$k = 1, \dots, N,$

j	Reaction	a_j	β_j	E_j
1	$O_3 + O \rightarrow O_2 + O + O$	6.76×10^6	2.50	1.01×10^{12}
2	$O_2 + O + O \rightarrow O_3 + O$	1.18×10^2	3.50	0.00
3	$O_3 + O_2 \rightarrow O_2 + O + O_2$	6.76×10^6	2.50	1.01×10^{12}
4	$O_2 + O + O_2 \rightarrow O_3 + O_2$	1.18×10^2	3.50	0.00
5	$O_3 + O_3 \rightarrow O_2 + O + O_3$	6.76×10^6	2.50	1.01×10^{12}
6	$O_2 + O + O_3 \rightarrow O_3 + O_3$	1.18×10^2	3.50	0.00
7	$O + O_3 \rightarrow 2O_2$	4.58×10^6	2.50	2.51×10^{11}
8	$2O_2 \rightarrow O + O_3$	1.88×10^6	2.50	4.15×10^{12}
9	$O_2 + O \rightarrow 2O + O$	5.71×10^6	2.50	4.91×10^{12}
10	$2O + O \rightarrow O_2 + O$	2.47×10^2	3.50	0.00
11	$O_2 + O_2 \rightarrow 2O + O_2$	5.71×10^6	2.50	4.91×10^{12}
12	$2O + O_2 \rightarrow O_2 + O_2$	2.47×10^2	3.50	0.00
13	$O_2 + O_3 \rightarrow 2O + O_3$	5.71×10^6	2.50	4.91×10^{12}
14	$2O + O_3 \rightarrow O_2 + O_3$	2.47×10^2	3.50	0.00

Table 1: Three-species, 14-step reaction mechanism for ozone decomposition [5]. Units of a_j are in appropriate combinations of cm, mol, s and K so that $\dot{\omega}_k$ has units of mol cm⁻³ s⁻¹; units of E_j are in erg mol⁻¹.

where $J = 14$ is the number of elementary reaction steps in the ozone decomposition reaction mechanism given in Table 1 and $N = 3$ is the number of species. The constant parameters a_j , β_j , E_j , ν'_{kj} , ν''_{kj} and \Re represent the kinetics rate constant of reaction j , the temperature dependence exponent of reaction j , the activation energy of reaction j , the stoichiometric coefficient of the k th species in reaction j of the reactants and products, and the universal gas constant ($\Re = 8.31441 \times 10^7$ erg mol⁻¹ K⁻¹), respectively. The system of Eqs. (9) are closed using the ideal gas equation of state

$$p_0 = \rho \Re T \sum_{k=1}^3 \frac{Y_k}{M_k}, \quad (15)$$

where $p_0 = 8.32 \times 10^5$ dynes/cm² is the constant pressure.

Following Margolis [5], the governing equations are simplified using the following assumptions and constants:

$$\mathcal{D}_1 = \mathcal{D}_2 = \mathcal{D}_3 = \mathcal{D}, \quad (16a)$$

$$\rho^2 \mathcal{D} = 4.336 \times 10^{-7} \text{ g}^2/(\text{cm}^4\text{-s}), \quad (16b)$$

$$\rho \lambda = 4.579 \text{ g}^2/(\text{cm}^2\text{-s}^3\text{-K}), \quad (16c)$$

$$c_p^1 = c_p^2 = c_p^3 = c_p = 1.056 \times 10^7 \text{ erg}/(\text{g-K}), \quad (16d)$$

$$M_1 = 16 \text{ g/mol}, \quad M_2 = 32 \text{ g/mol}, \quad (16e)$$

$$M_3 = 48 \text{ g/mol}, \quad (16e)$$

$$h_{01} = 1.534 \times 10^{11} \text{ erg/g}, \quad h_{02} = 0 \text{ erg/g},$$

$$h_{03} = 3.011 \times 10^{10} \text{ erg/g}. \quad (16f)$$

The initial and boundary conditions are applied in a frame of reference in which the fluid is initially at rest. A semi-infinite computational domain is considered

with the following boundary conditions

$$\frac{\partial T}{\partial \psi} = \frac{\partial Y_1}{\partial \psi} = \frac{\partial Y_2}{\partial \psi} = \frac{\partial Y_3}{\partial \psi} = 0, \quad (17)$$

for $\psi = 0, \infty$ and $t \geq 0$.

These conditions are equivalent to zero flux of thermal energy and species mass at $\psi = 0, \infty$, which also leads to $u(t, 0) = 0$, and hence, $\dot{m}_0 = 0$. Using these assumptions with a unity Lewis number as done in Margolis [5], and initial conditions and further reductions as described by Singh, *et al.* [4], we obtain a form suitable for numerical integration.

Results and Discussion

The steady state temperature profile and mass fraction distribution of O , O_2 and O_3 , in the ozone decomposition flame, are plotted in Fig. 1. It is

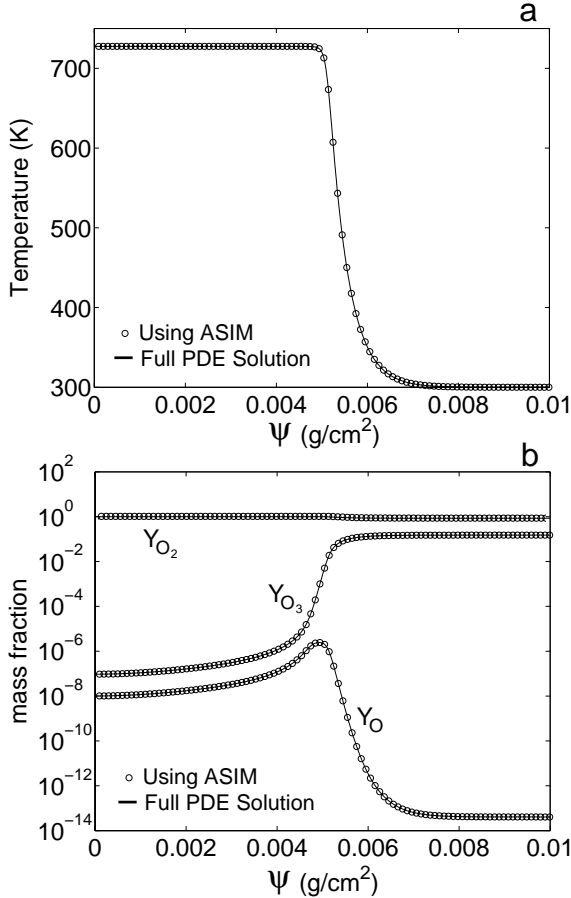


Figure 1: Ozone decomposition flame profile at $t = 4.115$ s for a) temperature, and b) species mass fractions.

seen that the steady profiles obtained when using the ASIM are nearly identical to those obtained by full integration.

Figure 2 compares the phase error in the solutions obtained by full integration, use of the ASIM, and the MPP method, all using a spatial resolution of 1000 grid points, relative to the baseline solution obtained by full integration at a spatial resolution of 10000 grid points. The numerical computations

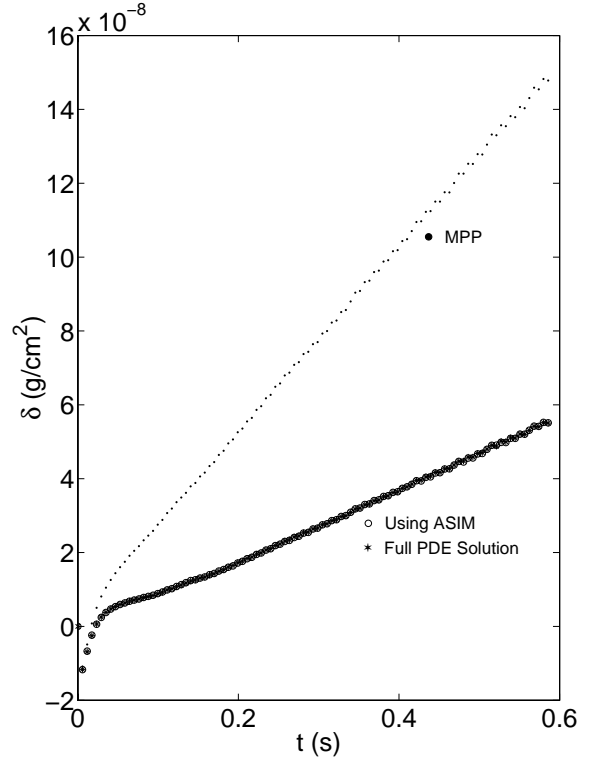


Figure 2: The phase error δ incurred in computations of the ozone laminar flame with the three methods, at a resolution of 1000 points, relative to computations using full integration at a resolution of 10000 points.

are done using second order, central difference approximations for spatial discretization and a second order backward difference formula (BDF) method, in the standard differential algebraic solver DASSL, for time advancement. Use of DASSL is not required for full integration, but is required when using the ASIM and the MPP methods for solving the resulting differential algebraic system of equations from spatial discretization. For error analysis all computations are done using the DASSL package with same time increments until steady state is achieved, in order to remove any numerical bias. The phase error δ for the solution obtained by the three methods and the baseline solution is measured as the Lagrangian distance between the location within the flame front where the mass fraction of O_3 is 0.075. There is a phase difference between the full integration at 1000 grid points

and the baseline solution due to the inherent phase error in the BDF numerical method used. This is depicted in Fig. 2 where stars represent the phase error in the full integration. At steady state the flame front propagates at a uniform speed, and the phase difference increases linearly, which signifies that different flame propagation speeds or burning rates are predicted at different grid resolutions. Near steady state, as can be seen from Fig. 2, the phase errors incurred when using the ASIM and full integration with the same resolution, are essentially identical. On the other hand the phase error incurred by the MPP method is substantially larger, resulting in an error in the prediction of flame propagation speed or the burning rate. This is evident from the difference in slopes of the phase error curve for the MPP method and the slope of the phase error curve when the ASIM or full integration is used.

Conclusions

While no robust analysis exists to determine convection and diffusion time scales *a priori*, we find that in reactive flow systems in which convection and diffusion have time scales comparable to those of reactions, MPP can lead to large transient and steady state errors. The error incurred when using the ASIM is much smaller than that in the MPP method. Using the ASIM, reaction, convection and diffusion are better coupled, while systematically equilibrating fast time scales. The ASIM is shown to be a good approximation for the long time dynamics of reactive flow systems. At this point the fast and slow subspace decomposition is dependent only on reaction and should itself be modified to account for convection-diffusion effects. In this work we have illustrated the improved accuracy in describing the slow dynamics of a simple reaction-diffusion systems when using the ASIM, with a concomitant decrease in computational cost.

Acknowledgments

This work has received support from the National Science Foundation under CTS-9705150, the Air Force Office of Scientific Research under F49620-98-1-0206, and Los Alamos National Laboratory.

References

- [1] Maas, U., and Pope, S. B., *Combust. Flame* 88: 239 (1992).
- [2] Maas U., and Pope, S. B., *Twenty-Fifth Symposium (International) on Combustion* The Combustion Institute, Pittsburgh, 1994, p. 1349.
- [3] Singh, S., Rastigejev, Y., Paolucci, S., and Powers, J. M., *Combust. Theory Model.* 5:163 (2001).
- [4] Singh, S., Powers, J. M., and Paolucci, S., *J. Chem. Phys.* 117: 1482, (2002).
- [5] Margolis, S. B., *J. Comp. Phys.* 27:410 (1978).